Peer-reviewed version available at *Insects* **2017**, *8*, , 51; doi:10.3390/insects8020051

Article

Estimating Density and Temperature Dependence of Juvenile Vital Rates Using a Hidden Markov Model

Robert M. McElderry [1,2,†]

[1] University of Miami, Coral Gables, FL 33146, USA
[2] Fairchild Tropical Botanic Garden, Miami, FL 33156, USA
† Current address: University of California, Los Angeles, CA 90095, USA; rmcelderry@ucla.edu

Abstract: Organisms in the wild have cryptic life stages that are sensitive to changing environmental conditions and can be difficult to survey. In this study, I used mark-recapture methods to repeatedly survey *Anaea aidea* (Nymphalidae) caterpillars in nature, then modeled caterpillar demography as a hidden Markov process to assess if temporal variability in temperature and density influence the survival and growth of *A. aidea* over time. Individual encounter histories result from the joint likelihood of being alive and observed in a particular stage, and I included hidden states by separating demography and observations into parallel and independent processes. I constructed a demographic matrix containing the probabilities of all possible fates for each stage, including hidden states, e.g., eggs and pupae. I observed both dead and live caterpillars with high probability. Peak caterpillar abundance attracted multiple predators, and survival of fifth instars declined as per capita predation rate increased through spring. A time lag between predator and prey abundance was likely the cause of improved fifth instar survival estimated at high density. Growth rates showed an increase with temperature, but the most likely model did not include temperature. This work illustrates how state-space models can include unobservable stages and hidden state processes to evaluate how environmental factors influence vital rates of cryptic life stages in the wild.

Keywords: *Anaea aidea*; caterpillar demography; multi-state mark-recapture; state-space model; stage-structured matrix

1. Introduction

All organisms have cryptic life stages, such as seed dormancy in plants, diapause in insects, and hibernation in mammals, but often non-dormant states such as breeding status or larval stages in fishes, amphibians, and arthropods are difficult study in the field. Compared to more apparent stages (i.e., adults), cryptic life stages are often more sensitive to environmental stressors such as climate change, resource limitation, and predation. Alterations in an organism's life stages and associated vital rates (i.e., survival, growth, and reproduction) can have dramatic effects on its spatial distribution and abundance. With an exponential increase in the listing of endangered species and loss of biodiversity globally [1], there is a critical need to quantify how environmental stressors influence all life stages and population dynamics. Cryptic stages, however, are often not incorporated in population dynamic studies, due in part to the difficultly of observing these stages in the field. Given that future environmental conditions (i.e., temperature and precipitation) are projected to increase in inter-annual variability over time, understanding how changing environmental factors influence cryptic life stages will become increasingly important over time.

Incorporating cryptic life stages into empirical demographic models is feasible and stems from a rich history of mark-recapture (MR) statistical procedures (see Appendix A). At the core of these statistical procedures is the evaluation of the joint likelihood of individuals surviving and being detected [2–5]. Multi-state mark-recapture (MSMR) models extended MR procedures to estimate stage-structured matrix models [6], which are popular tools in population biology to represent the life cycle of organisms with discrete life stages [7]. This link is important because a variety of analytical tools exist to extract demographic and life history properties from age or stage-structured matrices [7]

and these matrices are useful for predicting population viability [8]. More recently, MSMR analysis and stage-structured population matrix models are being evaluated using a class of models called state-space models (SSM)[9,10], effectively unifying all MR procedures[11,12]. Within a SSM, the state process and observation process are represented by two parallel time series and the joint likelihood of observing system in a particular state is given by the product of likelihoods for each process [11,12]. Perhaps the most appealing aspect of SSMs is the ability to model hidden states and hidden processes, e.g., Gimenez et al. [13] highlighted the use of hidden Markov models (HMM), a particular type of SSM, to include uncertainty in breeding status as a hidden state.

A HMM is an ideal tool to analyze MSMR data for organisms with stages that are hard to observe in the wild. A prime example of organisms with complex life cycles and cryptic life stages are Lepidoptera (butterflies and moths). Like many organisms, Lepidoptera undergo a series of discrete developmental stages. Newborns hatch from eggs, develop through five instars, and pupate before emerging as winged adults. A majority of the demographic studies of butterflies focus exclusively on the adult life stage, because juvenile stages are cryptic and small. Successful recruitment to the adult butterfly stage, however, is determined by juvenile survival and growth, which are sensitive to environment conditions. Identifying the environmental factors that influence juvenile dynamics is particularly important, from an applied perspective, for prioritizing restoration actions and cultivating persistence of rare and endangered butterflies on the brink of extinction [14,15].

Despite the clear relevance of juvenile stages for predicting adult fitness and overall population dynamics [15], few studies have included juvenile vital rates to evaluate rare insect population dynamics (but see [16,17]. The most commonly used method to assess how environmental factors influence the population dynamics of rare insects is to correlate environmental variables with the number of adult insects observed (e.g., [14,18–20]. This method searches for simple correlations between variables that result from multiple processes with complex interactions and feedback. However useful this method has been in rapid assessments and mining existing data sets, resulting models tend to lack statistical power and suffer from overfitting [21]. A mechanistic approach, in which specific vital rates are linked to environmental variables, appears a more promising means for evaluating environmental drivers of population dynamics (e.g., [22,23]).

In this study I used a HMM, utilizing Bayesian procedures, to quantify the survival and development of *Anaea aidea*,caterpillars from egg to pupation. Additionally, I quantified how underpinning environmental drivers influenced the temporal variation in these vital rates. *Anaea aidea* (Lepidoptera; Nymphalidae) was selected for this study, in part, to help develop a restoration plan for an endangered butterfly, *Anaea troglodyta floridalis*, which is phylogenetically and ecologically similar to *A. aidea* and currently too rare to be studied directly [24]. *Anaea t. floridalis* is endemic to the endangered pine rockland ecosystem of southern Florida where juvenile mortality of *A. t floridalis* exceeds 70% [25]. In concert with other environmental stressors, such as atypical frosts and an altered disturbance regime, high juvenile mortality may be a primary driver of *A. t floridalis* population decline [20]. However, few data exist that describe *A. t. floridalis* life history and sensitivities of vital rates to disturbance and the environment. To fill in this data gap, I monitored a complete recruitment pulse of *A. aidea* from the appearance of eggs to the emergence of adults during the spring, a time when temperatures steadily increase and caterpillar densities peak. To represent *Anaea*'s life cycle, I developed a periodic stage-structured matrix model of population dynamics that projects the population through multiple generations over one year in 3-day time steps (see [26]), and I describe here how I estimated the juvenile vital rates for this periodic model while testing each vital rate for the effects of temperature and conspecific density. I hypothesized that growth rates would increase over time as spring temperatures warmed, typical for exotherms, and that survival of all stages would increase during the recruitment period as warming spring temperatures reduce the chance of death due to cold and frost. I hypothesized alternatively that density-dependent effects could instead control survival (see [27], with high density[28] either attracting predators or resulting

in intraspecific competition for food, both of which would result in lower survival at high density. Conversely, high survival at high density may result from safety in numbers, predator satiation or dilution, or a time lag between prey and predator densities [29].

2. Materials and Methods

2.1. Study species and field methods

Anaea aidea (tropical leafwing) is distributed throughout Central America and Mexico in tropical dry forest [30], and a population has persisted many years in Austin, Texas, U.S.A., (Larry Gilbert, personal communication). I surveyed *A. aidea* on its local larval host plant, *Croton fruticulosus*, in 14 randomly selected (see Appendix A) host-containing plots at the University of Texas Brackenridge Field Laboratory (BFL), which comprises 82 acres along the Colorado River in Austin (30°17′00″N, 97°46′44″W). Suitable habitat at BFL was similar in appearance to habitats were *A. aidea* and *C. fruticulosus* were observed in larger, less-disturbed natural areas west of Austin, i.e., oak-cedar woodland on limestone outcrop upslope from riparian hardwood forest and meadows on alluvial terraces.

In each plot I searched each tagged *C. fruticulosus* shrub for *A. aidea* caterpillars at each of nine survey dates. Three days were required to survey all plots, so I resurveyed each plot every three days beginning 28-Mar-2011 and continued every day until 23-Apr-2011. All *A. aidea* caterpillars encountered were included in the survey, and I tracked each individual caterpillar through time recording its developmental stage (egg, 1 of 5 instars, or pupa), length, and status (live or dead) at each survey date. Mark-recapture of caterpillars is rare (but see [18,31]) since caterpillars shed their skins between developmental stages. However, the particular behavior of *A. aidea* caterpillars provided an opportunity for marking the leaf where they were found, so they could be relocated in subsequent surveys (see [16] and Appendix A for details). Typical of MR analyses, I arranged the string of observations for each caterpillar over all dates as an encounter history.

2.2. Model description

I represented all possible states (live, newly dead, dead) and stage (egg, first to fifth instar, or pupa) in a column stochastic model ($\boldsymbol{P}_X$) that describes all possible transitions among states and stages [9,13].

$$\boldsymbol{P}_X = \left[\begin{array}{c|c} J & Z \\ \hline M & U \end{array}\right] \tag{1}$$

The matrix, $\boldsymbol{P}_X$, is a block matrix consisting of matrices $\boldsymbol{J}$, $\boldsymbol{M}$, $\boldsymbol{Z}$, and $\boldsymbol{U}$, and contains the transition rules for a Markov process whereby an individual's current state and stage predict its future state and stage.

Matrix $\boldsymbol{J}$ represents probabilities of growth among juvenile stages that remain alive. Each element is a product of survival and growth and corresponds to an arrow in the life cycle graph for *A. aidea* juveniles (Figure 1). In 3-day time steps, there is a stage-specific probability of surviving, ϕ_i, and a stage-specific probability of growing from stage i to stage j, ψ_{ji}, independent of survival. Individuals can either remain in the same stage, $j = i$ (called stasis), grow to the next stage, $j = i + 1$, or early instars may grow two stages, $j = i + 2$.

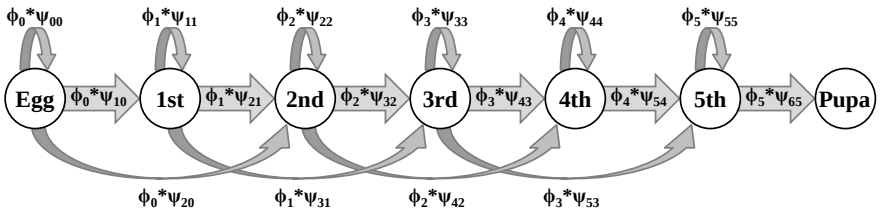

Figure 1. Diagram of the juvenile portion of the leafwing life cycle (*Anaea spp.*) with circles indicating each developmental stage, and arrows indicating the one time step probabilities of transitioning (ψ_{ji}) from stage i to stage j conditional on survival (ϕ_i).

Matrix $\boldsymbol{M}$ represents all possible transitions from live stages to newly dead stages, and utilizes the same stage-specific survival and growth probabilities. Living individuals at time t die with probability $1 - \phi[i]$ and are partitioned into newly dead stage classes, e.g., newly dead 1st instar, etc. I distinguished between newly dead and dead, because newly dead individuals can be encountered in the field, but quickly disappear. Similarly, newly dead individuals transition to the dead state, which is absorbing and is represented by the last row in matrix $\boldsymbol{M}$ [32].

The remaining two matrices, $\boldsymbol{Z}$ and $\boldsymbol{U}$, serve to enforce the absorbing state. Matrix $\boldsymbol{Z}$ and $\boldsymbol{U}$ have appropriate dimensions with all elements set to zero, which represents the impossibility of transitions from both dead states to the live state and transitions among newly dead stages. Elements in the last row of $\boldsymbol{U}$ are one and represent individuals in the newly dead state transitioning to the absorbing state.

While the block matrix $\boldsymbol{P}_X$ describes the underlying state process of interest, matrix $\boldsymbol{P}_O$ describes the parallel process by which I observe individuals. Matrix $\boldsymbol{P}_O$ contains the probabilities of being observed (p_i) for all live and dead stages along the sub-diagonal. The columns of $\boldsymbol{P}_O$ correspond to the true stage of an individual and the rows represent the possible stages in which an individual can be observed. The probability of not being observed is represented in the top row and is the complement of each stage-specific probability of being observed, i.e., $1 - p_i$ (for matrix details, Appendix B).

2.3. Vital rates and covariates

Survival in each stage i, $\phi[i]$, was modeled either as a constant, a function of survey date, or a function of caterpillar density. I used survey as an unspecified temporal effect to represent the myriad of changes occurring during spring, while density and temperature represent two specific covariates that change during spring. I represented caterpillar density at the individual plant level either as the number of caterpillars or the sum of all caterpillar lengths to account for caterpillar biomass (see Appendix A). These density metrics correspond to two mechanisms by which density dependence may be realized. Numbers of caterpillars may be an attractor for foraging predators, or could provide safety in numbers, given a constant number of predators. Increasing caterpillar biomass per plant shows not just an increase in numbers but also of caterpillar size, and larger caterpillars consume more foliar biomass than smaller caterpillars.

Growth from stage i to stage j, ψ_{ji}, was modeled either as a constant, a function of survey date, or a function of local air temperature. Temperature is known to affect development time in insects, with increasing temperature generally increasing rates of metabolism and consumption resulting in quicker development [33]. To quantify the effect of temperature on development time of *A. aidea*, I obtained air temperature data collected every hour for the Austin area from the National Weather Service [34] and averaged hourly temperatures over three day intervals corresponding to the survey intervals for each site. I used the logit link to for all survival functions and the multinomial logit for growth to allow for transitions to multiple stages while requiring that the sum of all possible transitions from i to any stage j sum to one (for details, Appendix C).

2.4. Model likelihood

Two equations comprise the likelihood of this hidden process model. The state equation describes the state of an individual at time t given its state at time $t-1$ and $\boldsymbol{P}_X$. The observation equation describes the probability of being observed at time t given the state of an individual at time t and $\boldsymbol{P}_O$.

$$\begin{aligned} \boldsymbol{X}_{k,t}|\boldsymbol{X}_{k,t-1} &\sim Categorical(\boldsymbol{P}_X\boldsymbol{X}_{k,t-1}) \\ \boldsymbol{Y}_{k,t}|\boldsymbol{X}_{k,t} &\sim Categorical(\boldsymbol{P}_O\boldsymbol{X}_{k,t}) \end{aligned} \tag{2}$$

Each individual k at each time $t-1$ was represented by a matrix $\boldsymbol{X}_{k,t-1}$ of zeros with a one in the row and column that indicates the state of the individual. The state of an individual at time t was predicted by the vector of probabilities obtained by multiplying $\boldsymbol{P}_X$ by $\boldsymbol{X}_{k,t-1}$. Similarly, the observed state of individual k was contained in matrix $\boldsymbol{Y}_{k,t}$. and the probability of being observed in each state given its actual state is obtained by multiplying $\boldsymbol{P}_O$ by $\boldsymbol{X}_{k,t}$. The categorical distribution is a special case of the multinomial distribution for a single sample and is appropriate here since these equations were evaluated for each individual at each time step.

I used Bayesian estimation via Markov chain Monte Carlo (MCMC) simulations to fit the equations above to encounter histories of marked caterpillars surveyed in the field. For linear model parameters, e.g., b_{0i}, a_{1i}, etc. describing survival and growth probabilities, I used uninformative normal prior distributions and uninformative uniform distributions between zero and one for observation probabilities. Demographic parameters for eggs and pupae, including the fifth instar to pupa transition, were rarely observed but necessary for model stability, so I estimated informative prior distributions using data from lab-reared larvae. The posterior distributions for all parameters were estimated using 10,000 MCMC iterations following 120,000 iterations of 'burn in', which according to standard convergence diagnostics was sufficient for model convergence. I performed all procedures using a high-performance computing cluster and the programs R (version 3.1.0 (2014-04-10) [35]) and JAGS [36], controlling JAGS via the R package, `rjags`.

Constructing 18 competing models I used Akaike's information criteria (AIC) to evaluate the relative support of candidate models [37]. Specifically, I investigated the effects of date and density on survival and the effects of date and temperature on growth. I also tested for reduced stage structure in survival, grouping first to fourth instars as distinct from fifth instars. In all models the probability of observation was stage-dependent and constant. It is important to note that I evaluated the relative fit of each complete demographic model rather than evaluating each vital rate-environment relationship independently. Each candidate demographic model contained a unique combination of vital rate-environment relationships, representing a competing hypothesis of environmental sensitivity integrated within the system's dynamics. With this approach, the relationship between each vital rate and the environment was evaluated in the context of all other vital rates.

3. Results

Caterpillar abundance increased during this study to a maximum density in mid-April, and then decreased as new individuals appeared less often and either died, left the host plant to pupate, or left the host plant and the study area (Figure 2C). Over 27 survey dates (9 surveys plot^{-1}), I observed 510 individuals in a total of 2,183 observations. I observed both live ($n = 2,062$ observations) and dead ($n = 107$) caterpillars with relatively high probability (Figure 3A), but I seldom observed eggs and pupae ($n = 14$). The probabilities of observing live individuals varied by stage, with third and fourth instars observed with a lower probability compared with first, second, and fifth instars, which may be due to the shift in perch construction behavior from frass chain to leaf roll during these intermediate instars. The probabilities of observing dead individuals were relatively high, but these probabilities dropped significantly for fourth instars and more so for fifth instars (Figure 3A). Caterpillar corpses

encountered most commonly showed signs of predation, i.e., a blackened and somewhat shriveled body at a single feeding point, but there were a few corpses found that died during the molting process. Failed molting was indicated by a persistent head capsule from the previous instar stuck over the mouthparts of the new instar head capsule.

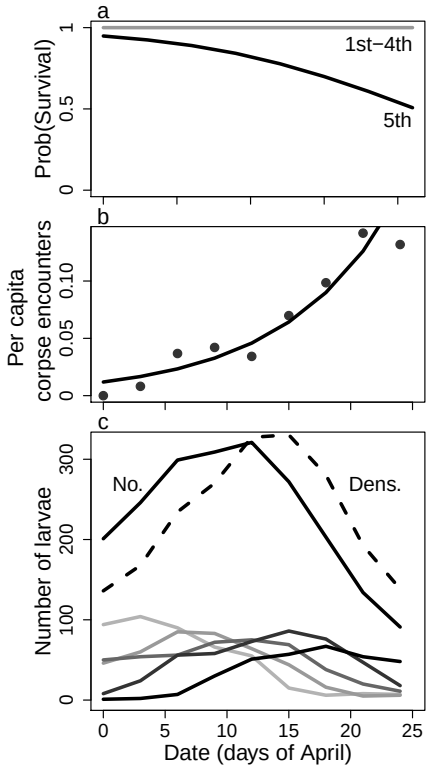

Figure 2. Change in (**a**) the mean probability of survival, (**b**) the per capita corpse encounter rate, and c) the number of larvae in each stage and total caterpillar biomass for *A. aidea* over the study period. Points in **b** represent the number of caterpillar corpses encountered per capita in each survey over the survey period, and the line represents the encounter rate; fit using Poisson regression. Upper lines in **c** show the total number of caterpillars (`No.`) and the size-scaled density (`Dens.`) over time, while the lower lines show the number of caterpillars in each instar. From light to dark, these lines represent early to late instars.

Survival of fifth instar larvae decreased over time, and relative model likelihood favored a simple model (Table S1) with early instars sharing one constant survival rate (Figure 2A). Survival started high for all stages, but steadily declined through the growing season for fifth instar larvae (Figure 2A). Survival appeared to be linked to density, but survival increased rather than decreased with high density (Figure S1). Models that used the size-scaled density (the summed length of caterpillars per plant) outperformed models that used the number of caterpillars per plant. For simplicity, only models with size-scaled density were used for model evaluation (Table S1). In general, density models did not receive significant support relative to other models. Mean caterpillar length, increased almost 5 fold during larval development from first to fifth instars (1st = 4.1, 2nd = 6.4, 3rd = 9.4, 4th = 13.3, 5th = 19.9 mm). Total size-scaled density lagged a few days behind the total number of caterpillars as each of these metrics increased to a maximum midway through the brood then decreased (Figure 2C). Over this time period, stage structure progressed from early instar predominance to late instar predominance.

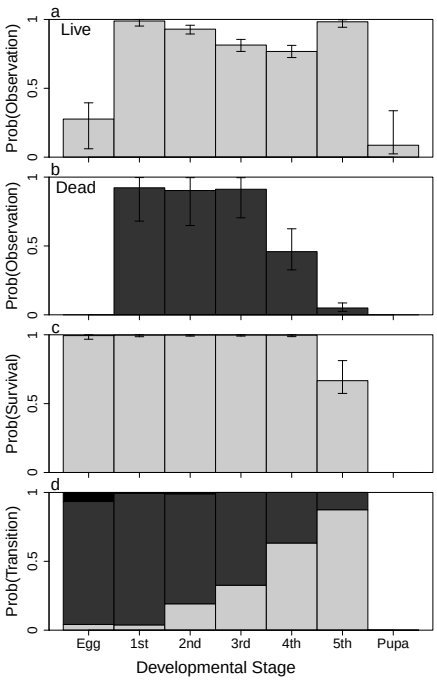

Figure 3. Stage-specific mean probabilities of (**a**) detection for live (light bars) and (**b**) dead (dark) individuals, (**c**) survival, and (**d**) transitioning from each stage i to either i (light), $i+1$ (medium), or $i+2$ (dark) during a 3-day interval for *A. aidea*, independent of survival. Error bars indicate the 95% credible interval.

Per capita predation rate, measured by Poisson regression of the number of corpses encountered over time, increasing by 11% per day during the month of April ($z = 7.32$, $p < 0.001$). Thus, individuals late in the brood had higher risk of predation than individuals early in the brood (Figure 2). Most dead caterpillars looked like they had been attacked by one of several insect or arachnid predators (i.e., the corpses were left clinging to the plant and exhibited evidence of feeding damage). I observed numerous hemolymph-sucking arachnid and hemipteran predators patrolling for caterpillars. Hemipteran predators included a wheel bug (Reduviidae) and a soldier bug (Pentatomidae), both of which hatched from eggs laid on *Croton* and appeared to focus on attacking *Anaea* caterpillars during each bug's larval development. Additional insects patrolling *Croton* and/or attacking *Anaea* caterpillars include green lacewings (Chrysopidae) and a small parasitoid wasp (Hymenoptera). Large polistine wasps (Polistinae) were seen searching *Croton*, and I observed several yellow jackets (Vespinae) attacking a large caterpillar of another species, but I did not observe predation events of *Anaea* caterpillars with these potential predators. Not observing predation by large predators such as wasps and birds does not mean that these predators did not have an effect. These predators tend to remove caterpillars from where they are found, leaving little if any trace (pers. obser.). There was a single instance where a rolled leaf shelter appeared chewed by a beak (triangular damage), leaving triangular markings and black hemolymph as the only remains. Predation rates by wasps and birds could not be quantified in this study. Disappearance of fifth instar larvae could mean either predation or pupation, but I controlled for this in the modeling by using an informative prior distribution for the probability of pupating.

The probability of growth (advancing either one or two stages) within 3 days decreased for progressively higher stages (Figure 3C). Concomitantly, the probability of remaining in the same stage for 3 days increases for later instars. Data for fifth instars pupating were insufficient to differentiate the posterior estimate from the prior distribution, so this description excludes fifth instars. Over the month of April, the probabilities of growth generally increased, mostly for early instars (Figure 4B). This increase in growth rates represents more rapid development and was linked

to increasing temperature (Figure 4). Temperatures showed a warming trend during this survey, increasing on average about 20◦F, but there was also significant temperature variation over time (Figure 4A). Warmer temperatures resulted in increased growth for all stages (Figure 4C). Despite a clear relationship between temperature and growth rates, model selection results suggested that neither temperature nor the progression of time in April were significant predictors compared with models that included only stage-dependent growth rates.

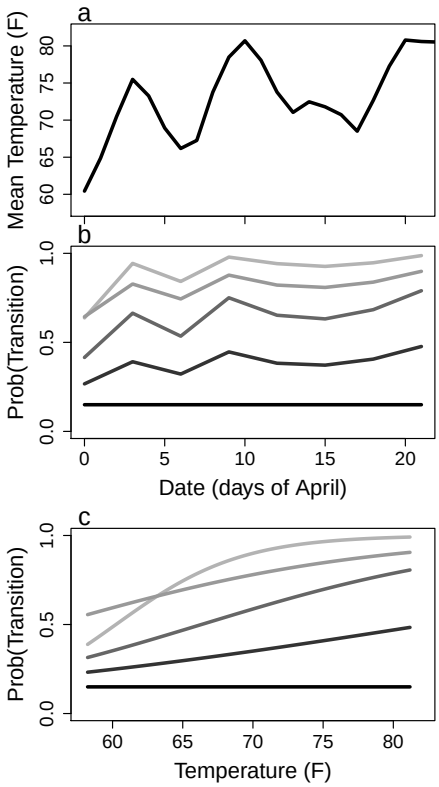

Figure 4. Change in (**a**) mean air temperature and (**b**) the probability of growing during a 3-day interval for *A. aidea* over the study period. The change in growth probabilities over time (**b**), is due to the relationship between transition probabilities and temperature (**c**). Temperature represents the hourly regional air temperature averaged over each 3-day time step. From light to dark, the lines in **b** and **c** represent early to late instars.

4. Discussion

Evaluating the sensitivity of cryptic life stages to environmental stressors is a major challenge as we develop conservation plans that account for climate change. Although we are often not able to monitor cryptic stages directly, SSMs easily incorporate hidden states and processes within demographic models and facilitate the evaluation of how changing environmental factors influence all life stages. My work displays the utility of SSMs in the study of cryptic life stages in a butterfly system, but this work is broadly applicable to any system with cryptic life stages. SSMs have been employed to reveal movement patterns of blue fin tuna [38], the importance of dormancy in mistletoes [39], to account for uncertainty in breeding status of roe deer, titis [13] and geese [40] and in the infection status for finches [41]. SSMs are a broad class of process models that include both Markovian and non-Markovian hidden processes, and this flexibility makes them especially useful for ecological modelling. For example, Schaub and Abadi [42], have developed a unified demographic modelling framework, called integrated population models, that uses a SSM to integrate time series count data with focused demographic data. Integrated population models will be particularly useful for insects to integrate field counts of a single life stage with laboratory data for all other stages to

obtain a complete empirical model of the life cycle and to evaluate within and between year trends. Integration of available data while considering each life stage and accounting for all sources of uncertainty is becoming increasingly important to understand how species will respond to future environmental conditions, especially for ectotherms (see [23]).

In this study, I applied a HMM using Bayesian procedures to estimate vital rates among juvenile stages from field surveys of caterpillars and I developed a stage-structured demographic matrix that describes the butterfly recruitment pulse, which is not well quantified in most butterfly demographic models [20,27]. In this state-space framework, I was able to clearly differentiate between the error in observation and state processes while including individual level covariates and data from multiple sources [11,12,43]. Variation in each vital rate was modeled via stochastic simulation (MCMC) for each individual at each survey (demographic stochasticity), independent of variation in observation probabilities and whether or not it was observed (observation error). Separating sources of error improved precision of demographic estimates and revealed patterns in the vital rates due to caterpillar density, temperature, and an unspecified temporal effect over the month of April.

Although survival appeared to increase at high caterpillar density, and growth rates increased at high temperatures, these relationships were not included in the best models. A benefit of using this approach is that the likelihood of all growth and survival probabilities for all stages and covariates were evaluated simultaneously, such that the effects of each vital rate-covariate relationship were tested within the context of the entire model, rather than testing each component independently before assembling the components [6]. Model selection using AIC suggested that the recruitment process for *A. aidea* was best represented either with stage-specific survival and growth rates constant over the month of April or with constant survival for early instars and decreasing survival for late instars over the month of April. This result does not suggest that density and temperature had no effect on the survival and growth rates of caterpillars but does indicate a simpler model was more efficient [37]. Although a stage-structured model of a Markovian process is appropriate for the discrete life cycle of butterflies, the inherent discretization of a continuous process, such as the time to each stage transition, may not be the best approach if the purpose of this research had been to explore temperature-dependence in growth rates (see discussion of Growth below).

4.1. Detection

Overall high observation probabilities for all living caterpillar stages and caterpillar corpses lend credibility to estimates of vital rates reported here. High observation probabilities estimated for caterpillar stages reflect the high fidelity of caterpillars to a particular area on a host plant, which was likely due to the time invested in building perches [16]. First to third instar larvae constructed frass chain perches extending from the leaf tip and generally remained on a single leaf for each stage. Third instars typically molted on the frass chain and then moved to a new leaf to construct a leaf roll as a fourth instar. This shift in perch types may explain why I observed third and fourth instars less frequently. Fourth and fifth instars rolled leaf shelters and fed in an increasing area around this shelter. As individuals grow progressively larger, they require more foliar biomass to complete development in each stage. To complete development in the laboratory, third, fourth, and fifth instars required approximately 2, 5, and 20 average sized leaves, respectively (unpublished data). Motivated by increasing nutritional requirements, later life stages became progressively more mobile in the field, and fifth instars created obvious signs of herbivory. Fifth instars often defoliated all or a large portion of leaves on their host plant and then moved to a new perch or host plant. Toward the end of the survey, host plants were increasingly defoliated and hungry caterpillars either moved to adjacent host plants or were not observed again.

Typical MR estimates of survival represents apparent survival, which is the joint probability of surviving and remaining in the survey area [5]. From the abundance of observed dead states I was able to estimate true survival (see [44]) and distinguished between developmental and predatory causes of death. Apparent survival was an issue for fifth instars. I found substantially fewer fifth

instar corpses, and all surviving fifth instars would eventually leave the host plant either in search of food or to pupate. Thus, fifth instars that disappeared from my surveys either survived and left in search of a pupation site, left in search of food and likely died, or died and the corpse was removed. I used a laboratory estimate of pupation probability (i.e., the probability of transitioning to a hidden stage) to decompose apparent survival and produce survival estimates for fifth instars in the field. In cases such as this with limiting data, demographic parameter estimates may not be identifiable [45], and unidentifiable parameters take the shape of the informative prior distributions in Bayesian models. In my study, egg development rate and probability of pupating were unidentifiable parameters due to the rarity of observing these hidden stages. I did not allocate time to searching for eggs, often hidden on the undersides of leaves, nor did I search for dead fifth instars or pupae on neighboring plants and leaf litter. Here, I incorporated data from lab-reared caterpillars, which is an efficient strategy for many insects and other short lived organisms. Doing so bolstered unidentifiable parameters, thus improving model stability and identifiability of confounded parameters, e.g., apparent survival.

4.2. Survival

Fifth instar survival declined over the study, suggesting a benefit to being born earlier. This brood was surveyed from the end of March to the end of April, a time during which spring progresses in Central Texas and several changes occur. The unspecified temporal effect I included in the model represents this spring progression. Warming temperatures is a primary driver of several other changes at this time, e.g., bud break, flowering, and the emergence of insects. In this study, it is likely that a subset of environmental factors, such as an increase in insect abundance [46] and/or increased nesting and breeding of predatory birds [47], was the driver of decreased survival of caterpillars during the month of April. Although, models that included density as a covariate received significantly less support than the time-dependent survival model, the complex relationship between density and survival may also help explain the mechanisms underlying the temporal decline in survival. Oviposition rate decreased and predation rate increased as the brood progressed. This trend may explain the observed initial increase in caterpillar density followed by the slow decrease over time. There are two ways density could have affected survival in this system (see [48]. Caterpillars increased in size and numbers, which decreased the amount of leaf tissue available for consumption. Similarly predator numbers and sizes seemed to increase in response to high caterpillar density, which could have resulted in an increase in the per capita predation rate.

The estimated effect of density on survival was interesting in that it implied that caterpillars were safer in high density, but unlike caterpillars that gain increased growth rates and reduced predation by feeding in aggregations (e.g.,[49]), *Anaea* caterpillars are solitary. Rather than caterpillars benefiting from safety in numbers, this result was better interpreted in terms of predator-prey dynamics with predator dilution or satiation at high prey density. In classic models of predator-prey dynamics, predator numbers lag behind prey numbers and predation rate increases with the rise in predator density [29]. Increasing numbers of predators coupled with decreasing prey numbers yields an increasing per capita death rate for the prey, which is what I found. The *Anaea* recruitment pulse was followed by a predator recruitment pulse, meaning that *A. aidea* caterpillars were threatened by fewer predators early in the brood, and predation pressure increased as the predator density increased over time.

The focus on predator-prey dynamics and positive density dependence ignores resource competition among prey and in fact appears to argue against the influence of limiting resources. However, the lack of support for negative dependence does not refute that it may have had an effect. In fact, I was unable to include the lasting effect of previous caterpillars in the metric of density employed here. While caterpillar density increased then decreased during the survey, none of the leaves consumed by caterpillars were replenished, meaning the abundance of edible leaves simply decreased over time. The abundance of leaves was not measured, but this resource certainly

Peer-reviewed version available at Insects 2017, 8, , 51; doi:10.3390/insects8020051

decreased in the month of April, possibly contributing to the observed decline in survival over time. Finding starved caterpillars would have supported this argument, but starving caterpillars would have wandered in search of food, making them almost impossible to find. Fifth instars were the most likely to starve, given their much higher nutritional needs relative to early instars, and were also the least likely to be observed dead. With the multiple complexities described here that may affect density dependence, it is not surprising that that caterpillar density was not supported in the preferred models. Caterpillar, predator, and leaf density are all likely to interact, and time was the only variable that seemed to effectively capture the change in these variables. Support for a temporal decline in survival over an effect of caterpillar density does not refute density dependence, rather it suggests that density dependence may be more complex than the simple linear function of density employed here.

The preeminence of predation as a cause of death for *A. aidea* juveniles is interesting not only for *A. aidea*, but it has implications for *A. t. floridalis*, for which a relatively large number of predators and parasitoids have been described [25]. What is interesting is that *A. t. floridalis* is the only leafwing that does not construct rolled leaf shelters as fourth and fifth instars. All other *Anaea* (and many closely related genera) construct shelters either by rolling single leaves or tying leaves together with silk, presumably to evade parasitism and predation [30]. *Anaea t. floridalis* larvae have been observed tying leaves together, but this behavior is observed very rarely [50], and may be due in part to the host plant architecture. The leaves of *Croton cascarilla* are generally too slender to roll and too sparsely arranged to tie multiple leaves together into a shelter, which is not the case for the leaves of *Croton* used by other *Anaea*. Without the protection of a leaf shelter, late instar *A. t. floridalis* are more exposed to predators, and the predation rates measured for *A. aidea* in this study likely underestimate those for *A. t. floridalis*. Indeed, predation/parasitism was listed as the most common cause of *A. t. floridalis* larval mortality in the field [25].

4.3. Growth

Growth rates were stage dependent and time-invariant, suggesting development time was not extremely variable over the month of April. As caterpillars develop, they grow larger and increase rates of feeding rates to meet increasing nutritional requirements for each successive molting [51]. With this fundamental development plan, the time required in each stage increases in later instars, represented here by increased probabilities of remaining in the same stage for each 3-day survey. The probability of growing two stages within 3 days was non-zero for early instars and was somewhat common only for eggs transitioning to first and second instars. Temperature appeared to affect development time, a phenomenon well described in ectothermic insects overall [51]. Increasing growth rates for first to fourth instars with warming spring temperatures indicated more rapid development later in the brood than early in the brood. Rapid development during a period of increased predation risk would be favorable. However, temperature-dependent growth rates were not supported over constant growth rates for each stage according to AIC. This finding likely stemmed from the discretization of a continuous process. In this framework the fate of an individual depends only on its current stage, and there is no memory of the stage duration for that individual. Temperature effects may have been diluted due to this feature, giving the result that a constant growth probability was more efficient.

5. Conclusions

This work contributes to the discussion of the drivers of population dynamics by analyzing density and temperature dependence within a comprehensive model of cohort dynamics while explicitly modeling individual stochasticity. Applying SSMs to analyze MSMR data is still relatively new and conveniently separates observation error from the demographic variability of interest. This level of detailed field observations and cohort model sophistication is unprecedented in butterfly research and has proven effective in illuminating the progression of individuals from

egg to pupa. This recruitment process is lacking from most butterfly and insect studies, but it is a crucial component when searching for links between 'noisy' time series of adult population counts and underlying demographic and climatic drivers. My work displays the utility of SSMs in estimating a stage-structured demographic matrix that includes hidden stages and the effect of climatic and demographic drivers, from time series data with missing observations. The many features offered by SSMs that I highlight here, make them particularly useful in studying life history and population dynamics in nature. This is especially true for insects, which are an exemplary example for organisms with low detectability and hidden states. State-space models are ideal for evaluating how environmental factors influence cryptic life stages of organisms. Quantifying the affects of environmental factors on cryptic life stage and populating dynamics will become increasingly important for accurately predicting how species will respond to environmental change (i.e., temperature and precipitation), which is projected to increase in inter-annual variability over time.

Supplementary Materials: The following are available online at www.mdpi.com/link, Figure S1: Density-dependent survival results, Table S1: Model selection results, Supplement S1: R code and data

Acknowledgments: Funding from the Lisa D. Anness Fellowship and the Department of Biology at the University of Miami supported this work. The University of Miami Center for Computational Science provided access to high-performance computing. I thank Lawrence E. Gilbert for suggesting the field protocol, and providing access to the Brackenridge Field Laboratory. Comments from Carol C. Horvitz, Joyce Maschinski, L.E. Gilbert, Donald L. DeAngelis, J. Albert C. Uy, and Lalasia Bialic-Murphy greatly helped the development of this manuscript. MDPI graciously waived the costs to publish in open access.

Author Contributions: R.M. conceived and designed the experiments, performed the experiments, analyzed the data, and wrote the paper.

Conflicts of Interest: The authors declare no conflict of interest. The founding sponsors had no role in the design of the study; in the collection, analyses, or interpretation of data; in the writing of the manuscript, and in the decision to publish the results.

Abbreviations

The following abbreviations are used in this manuscript:

MR	Mark-recapture
MSMR	Multi-state mark-recapture
SSM	State space model
HMM	Hidden Markov model
MCMC	Markov chain Monte Carlo
AIC	Akaike's information criteria
BFL	Brackenridge Field Laboratory

Appendix A. Study species and field methods

I mapped out all suitable habitat at BFL, defined as oak-cedar woodland on limestone outcrop, and overlaid it with a grid composed of 25-m $\times$ 25-m cells. Of 16 randomly selected grid points, 14 (22% of 71 total grid points) identified sites containing *C. fruticulosus* that were used for this study. I tagged each *C. fruticulosus* shrub within a contiguous patch at each site and searched each shrub for *A. aidea* caterpillars at each of nine survey dates. For each caterpillar found, I marked the leaf where it was perched with a letter unique within an individual plant, identifying the individual caterpillar. I marked leaves directly on the upper leaf surface with a permanent marker. All host plants in each patch were tagged and searched, so caterpillars that left in search of food most likely perished rather than crawling long distances to neighboring patches.

The particular behavior of *A. aidea* caterpillars provides an opportunity for MR studies (see [16]. Strong host fidelity and investment in constructed perches and shelters by these caterpillars facilitated re-sightings of caterpillars in marked locations on tagged host plants. Similar to other *Anaea* and closely related genera, e.g., Memphis and Consul, early instars web their feces, called frass, together into a chain that extends from the leaf tip [52–55]. This frass chain perch dangles from

the leaf, and is hypothesized to reduce predation risk via camouflage and/or predator free space [56]. Caterpillars abandon frass chains as they develop into later and larger instars and construct leaf shelters by either webbing leaves together or rolling single leaves [55]. When not feeding, caterpillars position themselves snugly in their rolled leaf, protecting their soft bodies from predators, leaving only their hard head capsules facing out (pers. obser.). Capitalizing on this behavior, I marked each caterpillar-inhabited leaf with a permanent marker and relocated each mark and its caterpillar during each survey.

As a measure of size, I measured the length of each caterpillar with a dial caliper, and the lengths of all caterpillars on an individual plant were summed to represent size-scaled density as a potential factor affecting caterpillar survival. Caterpillar length should scale with biomass but lacks a high degree of precision, because caterpillars can shorten or lengthen their bodies. Density on a single host plant is the relevant metric of density for this system because caterpillars generally stay on a single plant throughout their development and large caterpillars consume more resources than small ones.

Appendix B. Description of the demographic and observation matrices

The demographic matrix, $\boldsymbol{P}_X$, describes the underlying state process of interest, and is a block matrix consisting of matrices $\boldsymbol{J}$, $\boldsymbol{M}$, $\boldsymbol{Z}$, and $\boldsymbol{U}$. I used elements of the life cycle graph for the juvenile portion of the life cycle in the current model, and arranged only these probabilities for the juvenile stages in a matrix ($\boldsymbol{J}$);

$$\boldsymbol{J} = \begin{bmatrix} \phi_0\psi_{00} & 0 & 0 & 0 & 0 & 0 & 0 \\ \phi_0\psi_{10} & \phi_1\psi_{11} & 0 & 0 & 0 & 0 & 0 \\ \phi_0\psi_{20} & \phi_1\psi_{21} & \phi_2\psi_{22} & 0 & 0 & 0 & 0 \\ 0 & \phi_1\psi_{31} & \phi_2\psi_{32} & \phi_3\psi_{33} & 0 & 0 & 0 \\ 0 & 0 & \phi_2\psi_{42} & \phi_3\psi_{43} & \phi_4\psi_{44} & 0 & 0 \\ 0 & 0 & 0 & \phi_3\psi_{53} & \phi_4\psi_{54} & \phi_5\psi_{55} & 0 \\ 0 & 0 & 0 & 0 & 0 & \phi_5\psi_{65} & \phi_6 \end{bmatrix} \tag{3}$$

each column represents a particular stage at time t, each row represents the stage at time $t+1$, and each element j_{ji} represents the probability of survival and growth from stage i to stage j. Matrix $\boldsymbol{J}$ only represents transitions among living juvenile stages, but I also observed a large number of dead caterpillars.

Matrix $\boldsymbol{M}$ describes transitions from the live state to the dead state, and utilizes the same stage-specific survival and growth probabilities. Each element is a product of the probability of dying, $\mu_i = 1 - \phi_i$, and the probability of stage transitioning independent of the probability of dying, ψ_{ji}.

$$\boldsymbol{M} = \begin{bmatrix} \mu_0\psi_{10} & \mu_1\psi_{11} & 0 & 0 & 0 & 0 & 0 \\ \mu_0\psi_{20} & \mu_1\psi_{21} & \mu_2\psi_{22} & 0 & 0 & 0 & 0 \\ 0 & \mu_1\psi_{31} & \mu_2\psi_{32} & \mu_3\psi_{33} & 0 & 0 & 0 \\ 0 & 0 & \mu_2\psi_{42} & \mu_3\psi_{43} & \mu_4\psi_{44} & 0 & 0 \\ 0 & 0 & 0 & \mu_3\psi_{53} & \mu_4\psi_{54} & \mu_5 & 0 \\ \mu_0\psi_{00} & 0 & 0 & 0 & 0 & 0 & \mu_6 \end{bmatrix} \tag{4}$$

The probability of being dead and in stage i at time $t+1$ is given by the complement of survival given a caterpillar is in stage i at time t $(1-\phi_i)$ multiplied by the probability of growing from stage i to j (ψ_{ji}). Matrix $\boldsymbol{M}$ represents all possible transitions from live stages to dead stages, i.e., transitions independent of survival. Distinguishing the developmental stage of dead caterpillars allows this model to account for growth occurring between the last observation and death. Here the probability of growing from a fifth instar to a pupa then dying is equal to zero (element m_{66}).

Peer-reviewed version available at Insects 2017, 8, , 51; doi:10.3390/insects8020051

For both matrices, $\boldsymbol{M}$ and $\boldsymbol{J}$, the probability of growing from a pupa to an adult was set to zero. Pupae were rarely observed in the field and I was unable to collect data on pupa survival and the pupa to adult transition. The last row in matrix $\boldsymbol{M}$ represents individuals leaving the study, which is the absorbing state. In matrix $\boldsymbol{M}$, individuals enter the absorbing state by dying in a stage that left no visible remains, i.e., neither eggs nor pupae were observed in the dead state during this study.

The remaining two matrices within $\boldsymbol{P}_X$, $\boldsymbol{Z}$ and $\boldsymbol{U}$, serve to enforce the absorbing state. Matrix $\boldsymbol{Z}$ is has dimensions 7×6 (row $\times$ column) with all elements set to zero, which represents the impossibility of transitions from the dead state to the live state. Matrix $\boldsymbol{U}$ has dimensions 6×6 and represents stage transitions among dead stages, which are similarly impossible. All elements of $\boldsymbol{U}$ are set to zero except for the last row, which represents individuals in the dead state transitioning to the absorbing state. This model classifies dead individuals by developmental stage, and the newly dead state itself is not absorbing. When an individual dies, it moves to the newly dead state for one time step so that it may be observed dead. In the next time step, newly dead individuals move to the absorbing state, dead, indicating it has left the study. Individuals also entered the absorbing state by dying as either an egg or pupa, for which no visible remains were found.

The observation matrix, $\boldsymbol{P}_O$, describes the process by which we observe individuals.

$$\boldsymbol{P}_O = \begin{bmatrix} 1-p_0 & 1-p_1 & 1-p_2 & \dots & 1-p_{10} & 1-p_{11} & 1 \\ p_0 & 0 & 0 & \dots & 0 & 0 & 0 \\ 0 & p_1 & 0 & \dots & 0 & 0 & 0 \\ \vdots & \vdots & \vdots & \ddots & \vdots & \vdots & \vdots \\ 0 & 0 & 0 & \dots & 0 & 0 & 0 \\ 0 & 0 & 0 & \dots & p_{10} & 0 & 0 \\ 0 & 0 & 0 & \dots & 0 & p_{11} & 0 \end{bmatrix} \tag{5}$$

The columns of $\boldsymbol{P}_O$ correspond to the 13 state $\times$ stage categories [live(Egg, 1st, 2nd, 3rd, 4th, 5th, Pupa), newly dead(1st, 2nd, 3rd, 4th, 5th), dead] at time t. The rows of $\boldsymbol{P}_O$ represent the possible states and stages an individual can be observed as at time t [not observed, live(Egg, 1st, 2nd, 3rd, 4th, 5th, Pupa), newly dead(1st, 2nd, 3rd, 4th, 5th)]. The sub-diagonal of $\boldsymbol{P}_O$ contains the probabilities of being observed in stage i (p_i), given an individual is in stage i. The probability of not being observed is represented in the top row and is the complement of each state- and stage-specific probability of being observed, i.e., $1 - p_i$. Stage identification error was not included, so all other elements of $\boldsymbol{P}_O$ are equal to zero, because they represent being observed in a stage i when the individual is in fact not in stage i.

Appendix C. Logit transforms of survival and growth rates

I modeled the covariates for survival in each stage using a logit link, such that the log odds of surviving was equal to a linear function of each covariate.

$$logit(\phi_i) = b_{0k} + b_{1i}x \tag{6}$$

In this function, x was either an unspecified temporal effect or caterpillar density. Reducing this model by setting b_{1i} to zero I obtained the constant survival model.

Growth probabilities were modeled using a multinomial logit to allow for transitions to multiple stages while requiring that the sum of all possible transitions from i to any stage j sum to one.

$$\begin{aligned} \psi_{ii} &= [1 + exp(\alpha_{1i}) + exp(\alpha_{2i})]^{-1} \\ \psi_{i+1i} &= exp(\alpha_{1i})[1 + exp(\alpha_{1i}) + exp(\alpha_{2i})]^{-1} \\ \psi_{i+2i} &= exp(\alpha_{2i})[1 + exp(\alpha_{1i}) + exp(\alpha_{2i})]^{-1} \end{aligned} \tag{7}$$

The parameters α_{1i} and α_{2i} for each stage i are equal to the log odds of growing one or two stages, respectively, with respect to remaining in stage i. These two parameters estimate the three transition probabilities (growth one stage, growth two stages, and stasis), given the restriction that the probabilities sum to one ($\psi_{ii} = 1 - \psi_{i+1i} - \psi_{i+2i}$). To test for environmental effects, I formulated each parameter α_{1i} and α_{2i} as a linear function of x,

$$\begin{aligned} \alpha_{1i} &= a_{1i} + a_{xi}x \\ \alpha_{2i} &= a_{2i} + a_{xi}x \end{aligned} \tag{8}$$

where x was either an unspecified temporal effect or air temperature, and a_{xi} describes the slope of the relationship between α and x, which is equal for both α_{1i} and α_{2i}. Setting a_{xi} to zero reduces this model so that growth probabilities are constant. For certain transitions (fourth to fifth and fifth to pupa), the probability of growing two stages is zero, so the binomial logit was used for these probabilities with only two possible outcomes.

References

1. IUCN. The IUCN red list of threatened species. http://wwwiucnredlistorg/about/summary-statistics, 2013.
2. Cormack, R. Estimates of survival from the sighting of marked animals *Biometrika* **1964**, *51*, 429-438.
3. Jolly, G. Explicit estimates from capture-recapture data with both death and immigration-stochastic model *Biometrika* **1965**, *52*, 225-247.
4. Seber, G.A.F. A note on the multiple-recapture census. *Biometrika* **1965**, *52*, 249-259.
5. Lebreton, J.-D.; Burnham, K.P.; Clobert, J.; Anderson, D.R. Modeling survival and testing biological hypotheses using marked animals: a unified approach with case studies *Ecological Monographs* **1992**, *62*, 67-118.
6. Nichols, J.D.; Sauer, J.R.; Pollock, K.H.; Hestbeck, J.B. Estimating transition probabilities for stage-based population projection matrices using capture recapture data *Ecology* **1992**, *73*, 306-312.
7. Caswell, H. *Matrix population models: construction, analysis, and interpretation*; Sinauer Associates: Sunderland, Massachussetts, U.S.A., 2001.
8. Morris, W.; Doak, D. *Quantitative conservation biology: theory and practice of population viability analysis*. Sinauer Associates: Sunderland, U.S.A., 2002.
9. Fujiwara, M.; Caswell, H. Estimating population projection matrices from multi-stage mark-recapture data *Ecology* **2002**, *83*, 3257-3265.
10. Caswell, H.; Fujiwara, M. Beyond survival estimation: mark-recapture, matrix population models, and population dynamics *Animal Biodiversity and Conservation* **2004**, *27*, 471-488.
11. Buckland, S.; Newman, K.; Thomas, L.; Koesters, N. State-space models for the dynamics of wild animal populations *Ecological Modelling* **2004**, *171*, 157-175.
12. Thomas, L.; Buckland, S.T.; Newman, K.B.; Harwood, J. A unified framework for modelling wildlife population dynamics *Australian & New Zealand Journal of Statistics* **2005**, *47*, 19-34.
13. Gimenez, O.; Lebreton, J.-D.; Gaillard, J.-M.; Choquet, R.; Pradel, R. Estimating demographic parameters using hidden process dynamic models *Theoretical Population Biology* **2012**, *82*, 307-316.
14. Schultz, C.B.; Crone, E.E.Burning prairie to restore butterfly habitat: a modeling approach to management tradeoffs for the Fender's blue. *Restor Ecol* **1998**, *6*, 244-252.
15. Saastamoinen, M.; Ikonen, S.; Wong, S.C.; Lehtonen, R.; Hanski, I. Plastic larval development in a butterfly has complex environmental and genetic causes and consequences for population dynamics *Journal of Animal Ecology* **2013**, *82*, 529-539.
16. Caldas, A. Population ecology of Anaea ryphea (Nymphalidae): Immatures at Campinas, Brazil *J Lepid Soc* **1995**, *49*, 234-245.
17. Nakajima, M.; Boggs, C.L.; Bailey, S.; Reithel, J.; Paape, T. Fitness costs of butterfly oviposition on a lethal non-native plant in a mixed native and non-native plant community *Oecologia* **2013**, *172*, 823-832.
18. Young, A.M.; Moffett M.W. Studies on the population biology of the tropical butterfly Mechanitis isthmia in Costa Rica *American Midland Naturalist* **1979**, *101*, 309-319.

19. Harrison, P.J.; Hanski, I.; Ovaskainen, O. Bayesian state-space modeling of metapopulation dynamics in the Glanville fritillary butterfly *Ecological Monographs* **2011**, *81*, 581-598.
20. McElderry, R.M.; Salvato, M.H.; Horvitz, C.C. Population viability models for an endangered endemic subtropical butterfly: effects of density and fire on population dynamics and risk of extinction *Biodiversity and Conservation* **2015**, *24*,1589-1608.
21. Knape, J.; de Valpine, P. Effects of weather and climate on the dynamics of animal population time series *Proceedings of the Royal Society of London B: Biological Sciences* **2011**, *278*, 985-992.
22. Boggs, C.L.; Inouye, D.W. A single climate driver has direct and indirect effects on insect population dynamics *Ecology Letters* **2012**, *15*, 502-508.
23. Radchuk, V.; Turlure, C.; Schtickzelle, N. Each life stage matters: the importance of assessing the response to climate change over the complete life cycle in butterflies *Journal of Animal Ecology* **2013**, *82*, 275-285.
24. Salvato, M.H.; Salvato, H.L. Notes on the status and ecology of Anaea troglodyta floridalis (Nympalidae) in Everglades National Park *J Lepid Soc* **2010**, *64*, 91-97.
25. Salvato, M.H.; Salvato, H.L. Parasitism of the Florida leafwing and Bartram's hairstreak butterlfy immature stages. Comprehensive Annual Report to Everglades National Park, 2012.
26. Coll, C.; Horvitz, C.C.; McElderry, R. Stage-structured periodic population model for the Florida leafwing. *Int J Complex Systems in Science* **2012**, *2*, 1-5.
27. Nowicki, P.; Bonelli, S.; Barbero, F.; Balletto, E. Relative importance of density-dependent regulation and environmental stochasticity for butterfly population dynamics *Oecologia* **2009**, *161*, 227-239.
28. Berryman, A.; Stenseth, N.C.; Isaev, A. Natural regulation of herbivorous forest insect populations *Oecologia* **1987**, *71*, 174-184.
29. Roughgarden, J. *Primer of ecological theory*; Prentice Hall, Upper Saddle River, U.S.A., 1998.
30. Scott, J.A. *The butterflies of North America: a natural history and field guide*; Stanford University Press: Stanford, U.S.A., 1992.
31. Weseloh, R.M. Dispersal, survival, and population abundance of gypsy moth, Lymantria dispar (Lepidoptera: Lymantriidae), larvae determined by releases and mark-recapture studies *Annals of the Entomological Society of America* **1985**, *78*, 728-735.
32. Servanty, S.; Converse, S.J.; Bailey, L.L. Demography of a reintroduced population: moving toward management models for an endangered species, the whooping crane *Ecological Applications* **2014**, *24*, 927-937.
33. Wagner, T.L.; Wu H.-I.; Sharpe, P.J.; Schoolfield, R.M.; Coulson, R.N. Modeling insect development rates: a literature review and application of a biophysical model *Annals of the Entomological Society of America* **1984**, *77*, 208-220.
34. NOAA NWS. Weather observations for the past three days. (http://w1.weather.gov/data/obhistory/KATT.html 28 March - 1 May 2011). Austin Camp Mabry. Austin, U.S.A., 2011.
35. R Core Team. R: A language and environment for statistical computing, version 3.1.0 (2014-04-10) edn. R Foundation for Statistical Computing, Vienna, Austria, 2014.
36. Plummer, M. JAGS: A program for analysis of Bayesian graphical models using Gibbs sampling. In *Proceedings of the 3rd International Workshop on Distributed Statistical Computing*; 2003; pp 20-22.
37. Burnham, K.P., Anderson, D.R. *Model selection and multimodel inference: a practical information-theoretic approach*. Springer: New York, U.S.A., 2002.
38. Patterson, T.A.; Basson, M.; Bravington, M.V.; Gunn, J.S. Classifying movement behaviour in relation to environmental conditions using hidden Markov models *Journal of Animal Ecology* **2009**, *78*, 1113-1123.
39. McElderry, R.M.; Duquesnel, J.A.; Maschinski, J. Gauging reintroduction success with a hidden Markov model and analysis of transient dynamics *Conservation Biology* **In Review**.
40. Pradel, R. Multievent: an extension of multistate capture–recapture models to uncertain states *Biometrics* **2005**, *61*, 442-447.
41. Conn, P.B.; Cooch, E.G. Multistate capture–recapture analysis under imperfect state observation: an application to disease models *Journal of Applied Ecology* **2009**, *46*, 486-492.
42. Schaub, M.; Abadi, F. Integrated population models: a novel analysis framework for deeper insights into population dynamics. *Journal of Ornithology* **2011**, *152*, 227-237.
43. Gimenez, O.; Rossi, V.; Choquet, R.; Dehais, C.; Doris, B.; Varella, H.; Vila, J.-P.; Pradel, R. State-space modelling of data on marked individuals *Ecological Modelling* **2007**, *206*, 431-438.

44. Burnham, K.P. A theory for combined analysis of ring recovery and recapture data. In *Marked individuals in the study of bird population*; Lebreton, J., North, P., Eds.; Birkhauser Vet-lag: Basel, Switzerland, 1993; pp 199-213.
45. Schnute, J.T. A general framework for developing sequential fisheries models. *Canadian Journal of Fisheries and Aquatic Sciences* **1994**, *51*, 1676-1688.
46. Lowman, M.D. Seasonal variation in insect abundance among three Australian rain forests, with particular reference to phytophagous types *Australian Journal of Ecology* **1982**, *7*, 353-361.
47. Schwartz, M.D.; Reiter, B.E. Changes in North American spring International. *Journal of Climatology* **2000**, *20*, 929-932.
48. Dempster, J. The natural control of populations of butterflies and moths *Biological Reviews* **1983**, *58*, 461-481.
49. Clark, B.R.; Faeth, S.H. The consequences of larval aggregation in the butterfly *Chlosyne lacinia*. *Ecological Entomology* **1997**, *22*, 408-415.
50. Salvato, M.; Salvato, H.; Sadle, J. Tent building by larval Anaea troglodyta floridalis (Nymphalidae) *News of the Lepidopterists Society* **2015**, *57*
51. Chown, S.L.; Nicolson, S. *Insect physiological ecology: mechanisms and patterns*; Oxford University Press: Oxford, England, 2004.
52. Caldas, A. Biology of Anaea ryphea (Nymphalidae) in Campinas, Brazil *J Lepid Soc* **1994**, *48*, 248-257.
53. Muyshondt, A. Notes on the life cycle and natural history of butterflies of El Salvador. III. Anaea (Consul) fabius (Nymphalidae) *J Lepid Soc* **1974**, *28*, 81-99.
54. Muyshondt, A. Notes on the life cycle and natural history of butterflies of El Salvador. IV. Anaea (Memphis) eurypyle confusa (Nymphalidae) *J Lepid Soc* **1974**, *28*, 306-314.
55. Ramos, S.J. Notes on the life cycle and biology of Anaea troglodyte borinquenalis (Lepidoptera: Apaturidae) *Caribbean Journal of Science* **1984**, *20*, 19-24.
56. DeVries, P.J. *The butterflies of Costa Rica and their natural history vol I*; Princeton University Press: Princeton, U.S.A., 1987.